Crystal Structure of KPC-2: Insights into Carbapenemase Activity in Class A β-Lactamases[†,‡]

Wei Ke,[§] Christopher R. Bethel,[||] Jodi M. Thomson,[⊥] Robert A. Bonomo,[||,⊥] and Focco van den Akker*[,§]

Department of Biochemistry and Pharmacology, Case Western Reserve University, Cleveland, Ohio 44106, and Research Service, Louis Stokes Cleveland Veterans Affairs Medical Center, Cleveland, Ohio 44106

Received February 13, 2007; Revised Manuscript Received March 8, 2007

ABSTRACT: β-Lactamases inactivate β-lactam antibiotics and are a major cause of antibiotic resistance. The recent outbreaks of *Klebsiella pneumoniae* carbapenem resistant (KPC) infections mediated by KPC type β-lactamases are creating a serious threat to our "last resort" antibiotics, the carbapenems. KPC β-lactamases are serine carbapenemases and are a subclass of class A β-lactamases that have evolved to efficiently hydrolyze carbapenems and cephamycins which contain substitutions at the α-position proximal to the carbonyl group that normally render these β-lactams resistant to hydrolysis. To investigate the molecular basis of this carbapenemase activity, we have determined the structure of KPC-2 at 1.85 Å resolution. The active site of KPC-2 reveals the presence of a bicine buffer molecule which interacts via its carboxyl group with conserved active site residues S130, K234, T235, and T237; these likely resemble the interactions the β-lactam carboxyl moiety makes in the Michaelis−Menten complex. Comparison of the KPC-2 structure with non-carbapenemases and previously determined NMC-A and SME-1 carbapenemase structures shows several active site alterations that are unique among carbapenemases. An outward shift of the catalytic S70 residue renders the active sites of the carbapenemases more shallow, likely allowing easier access of the bulkier substrates. Further space for the α-substituents is potentially provided by shifts in N132 and N170 in addition to concerted movements in the postulated carboxyl binding pocket that might allow the substrates to bind at a slightly different angle to accommodate these α-substituents. The structure of KPC-2 provides key insights into the carbapenemase activity of emerging class A β-lactamases.

Carbapenems (imipenem, meropenem, and ertapenem) are the "last resort" β-lactam antibiotics for treating serious infections caused by multi-drug resistant Gram-negative bacteria. Unfortunately, the acquisition of carbapenem-hydrolyzing β-lactamases by bacteria has resulted in a major threat to the clinical utility of these compounds (*1*, *2*). Currently, the *Klebsiella pneumoniae* carbapenemases (KPC[1] type β-lactamases) are rapidly emerging as a major threat in the New York area (*3*−*5*), in Pennsylvania (*6*), and internationally (*7*, *8*). Three KPC variants have been found so far (KPC-1,-2, and -3), KPC-1 and KPC-2 being almost indistinguishable, whereas KPC-3 exhibits different hydrolytic properties (*9*).

KPC carbapenemases belong to the Ambler class A β-lactamases (EC 3.5.2.6) (*10*, *11*). In common with other class A β-lactamases, these highly proficient class A enzymes have an efficient hydrolysis "machinery" involving a catalytic serine residue (S70), which acylates β-lactam substrates, and a well-positioned deacylation water. S70 is involved in the nucleophilic attack at the carbonyl carbon of the substrate, leading to cleavage of the bond with the β-lactam ring nitrogen for penicillin and other substrates (Figure 1). The deacylation water molecule is primed by E166 and N170 for nucleophilic attack of the β-lactam−acyl-enzyme intermediate and serves to liberate the β-lactam substrate from the active site by deacylation. Both acylation and deacylation involve a nucleophilic attack which is facilitated by a correctly positioned oxyanion hole (formed by the backbone nitrogens of residues 70 and 237) that attracts the carbonyl oxygen atom. These described active site elements are supported by a complex hydrogen bonding network involving a pair of conserved lysines (K37 and K234), N132, and S130.

Serine carbapenemases such as KPCs are unique among the class A β-lactamases because of their ability to hydrolyze β-lactams containing a substituent at the α-position of the carbon atom in the β-lactam ring adjacent to the carbonyl (*12*, *13*). Examples of such β-lactams readily hydrolyzed by carbapenemases include imipenem (a carbapenem containing a 6α-hydroxyethyl moiety) but also cefoxitin (a cephamycin

[†] R.A.B. is supported by the Merit Review Program and NIH Grant R01AI063517-01. J.M.T. is supported by NIH Grant T32 GM07250 and the Case Medical Scientist Training Program. F.v.d.A. is supported by NIH Grant AI062968.

[‡] Coordinates and structure factors for the KPC-2 structure have been deposited with the Protein Data Bank (PDB entry 2OV5).

* To whom correspondence should be addressed: Department of Biochemistry RT500, School of Medicine, Case Western Reserve University, 10900 Euclid Ave., Cleveland, OH 44106-4935. Phone: (216)368-8511. Fax: (216)368-3419. E-mail: focco.vandenakker@case.edu.

[§] Department of Biochemistry, Case Western Reserve University.

[||] Louis Stokes Cleveland Veterans Affairs Medical Center.

[⊥] Department of Pharmacology, Case Western Reserve University.

[1] Abbreviations: KPC, *Klebsiella pneumoniae* carbapenemase; rmsd, root-mean-square deviation.

10.1021/bi700300u CCC: $37.00
Published on Web 04/19/2007

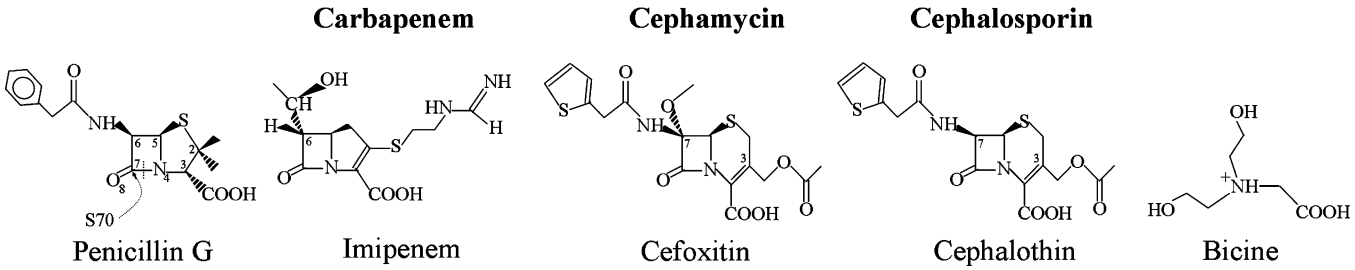

FIGURE 1: Schematic diagram of penicillin G, a carbapenem (imipenem), cephamycin (cefoxitin), a cephalosporin (cephalothin), and bicine. The bond that is broken during the acylation step involving S70's nucleophilic attack (curved gray dotted arrow) is shown for only penicillin G (straight dotted gray line between C7 and N4).

containing a 7α-O-CH_3 group) (Figure 1) (*9*, *12*, *13*). Previous crystallographic studies of the class A serine carbapenemases NMC-A and SME-1 did not yield a unified conclusion with regard to their carbapenemase activity. Interpretation of the NMC-A structure suggested a role for the slightly shifted position of N132 to perhaps accommodate these α-substituents (*12*, *14*), whereas the SME-1 structure suggested a needed conformational change for catalysis and importance for the C69−C238 disulfide, being in the proximity of the active site (*13*). Mutagenesis studies of the C69−C238 residues in SME-1 confirmed the critical role of this disulfide bond, but its function was not limited to carbapenemase activity since its disruption caused loss of hydrolytic activity toward all β-lactam antibiotics (*15*). On the basis of mutagenesis studies, Majiduddin and Palzkill (*16*) concluded that no single residue within the active site of SME-1 is solely responsible for carbapenemase activity and that this activity is likely due to multiple simultaneous substitutions and accompanying conformational rearrangements that prime the active site to accommodate and hydrolyze carbapenems and cephamycins.

The unresolved structural basis of this carbapenemase activity seen in class A enzymes and the urgent clinical threat presented by KPC β-lactamases found in *Klebsiella*, *Enterobacter*, and *Salmonella* spp. prompted our investigation of KPC-2. We present here the structure of KPC-2 determined to 1.85 Å resolution. Our analysis of KPC-2 in comparison to other class A β-lactamase enzymes reveals alterations in active site topology with respect to non-carbapenemases such as SHV-1 and TEM-1 that could rationalize the structural basis of carbapenemase activity. Furthermore, the active site of KPC-2 contains a well-resolved bicine molecule with its carboxyl moiety occupying a space that is likely involved in recognizing the carboxyl moiety of β-lactams, thus providing insights into substrate recognition.

MATERIALS AND METHODS

The KPC-2 β-lactamase is expressed using the pBR322-*cat*I-*bla*KPC-2 vector in *Escherichia coli* DH10B cells (a kind gift of F. Tenover, Centers of Disease Control and Prevention, Atlanta, GA). The plasmid containing bla_{KPC-2} was described by Yigit et al. (*17*) and has been confirmed by DNA sequencing. Transfected cells were grown in 500 mL of Luria-Bertaini (LB) broth containing 20 μg/mL chloramphenicol for 18 h and pelleted by centrifugation (5000*g* for 15 min). Cell pellets were resuspended in 20 mM Tris-HCl (pH 7.0), and periplasmic proteins were released using stringent periplasmic fractionation with lysozyme and EDTA as previously described (*18*). The supernatant was filter sterilized and passed through a phenylboronate column (MoBiTec), which has a specific binding affinity for class A β-lactamases, and KPC-2 was eluted using 0.5 M boronate and 0.5 M NaCl (pH 7.0). The eluent was loaded on a Superdex 75 size exclusion column, and fractions containing nitrocefin hydrolyzing activity were pooled and concentrated to 13 mg/mL in 10 mM Tris-HCl buffer (pH 7.6) (protein concentration measured using the Bradford method). The homogeneity of KPC-2 was estimated to be ~99% as assessed by SDS−PAGE. Carbapenemase activity was confirmed by hydrolysis of imipenem (imipenem $\lambda = 299$; $\Delta\epsilon = -9000\ M^{-1}\ cm^{-1}$).

Initial crystallization screens were carried out using the Grid PEG6000 screen kit (Hampton Research Inc.), resulting in small needle crystal clusters. Crystallization conditions were optimized; diffraction quality KPC-2 crystals could be obtained using the sitting drop method, and 0.7 μL of protein solution was mixed with 0.3 μL of reservoir solution and equilibrated against a reservoir solution containing 16% PEG6000 in 0.1 M bicine (pH 9.0). Crystals grew to full size in 3−14 days.

For crystallographic data collection, a single crystal was transferred to mother liquor containing 15% glycerol for 1 min, after which the crystal was flash-frozen in liquid nitrogen. A 1.85 Å resolution diffraction data set was collected at APS beamline 19BM at 100 K. The crystals belong to trigonal space group $P3_1$ with the following cell parameters: $a = 116.245$ Å, $b = 116.245$ Å, $c = 52.001$ Å, $\alpha = 90°$, $\beta = 90°$, and $\gamma = 120°$. The diffraction data were integrated and scaled using HKL2000 (*19*) (see Table 1 for processing statistics).

The KPC-2 structure was determined by molecular replacement using PHASER (*20*) with chain A of the SME-1 structure [PDB entry 1DY6 (*13*)] as the initial search model. PHASER found three molecules in the asymmetric unit, resulting in a solvent content of 47%. The top solution underwent several rounds of REFMAC (*21*) refinement and manual model building with COOT (*22*) which resulted in R and R_{free} values of 27.1 and 33.2%, respectively. The inability to further improve the R factors suggested a possible twinning problem which was confirmed using the Crystal Twinning Server (*23*). Subsequent refinement was carried out using CNS (*24*) with twinning operation "h,−h−k,−l" and twinning fraction 0.420. Simulated annealing refinement followed by temperature factor refinement and manual model building lowered the R factors considerably. No noncrystallographic symmetry restraints were used in refinement due to the relatively high resolution of the diffraction data. Electron density was of excellent quality for most of the

Table 1: Data Collection and Refinement Statistics for the KPC-2 Structure

data collection	
space group	$P3_1$
unit cell dimensions	$a = 116.25$ Å, $b = 116.25$ Å, $c = 52.00$ Å, $\alpha = 90°$, $\beta = 90°$, $\gamma = 120°$
wavelength (Å)	0.97
resolution (Å)	30−1.85 (1.92−1.85)
redundancy	3.2
data cutoff (σ)	−3.0 (default)
no. of unique reflections	64107
$\langle I\rangle/\langle\sigma(I)\rangle$	19.7 (2.3)
R_{merge} (%)	6.4 (34.4)
completeness (%)	95.6 (90.8)
refinement	
resolution range (Å)	30−1.85 (1.93−1.85)
no. of atoms in asymmetric unit	6174
R (%)	14.9 (24.9)
R_{free} (%)	19.0 (26.0)
rmsd from ideality	
bond lengths (Å)	0.0065
angles (deg)	1.29
average temperature factor (Å^2)	
protein	25.6
bicine	35.3
waters	26.6
Ramachandran plot statistics (%)	
most favored regions	90.2
additional allowed regions	9.2
generously allowed regions	0.6
disallowed regions	0

residues (see Figure 2A for representative density near one of the active sites). Throughout the refinement, electron density for a bicine buffer molecule in each of the three KPC-2 molecules was apparent (Figure 2B). Therefore, three bicine buffer molecules were included in refinement as well as 294 water molecules and the final model containing residues 30−292 for each molecule (see Table 1 for additional details). The progress of crystallographic refinement was monitored using DDQ (*25*), and the final model quality was assessed using PROCHECK (*26*).

RESULTS

The structures of three KPC-2 molecules present in the asymmetric unit are refined to R and R_{free} values of 14.8 and 19.0%, respectively, and 90% of the residues had ϕ and ψ angles in the acceptable region of the Ramanchandran plot (Table 1 and Figure 3A). Each molecule contains one *cis*-peptide (residue 167) which is common among other class A β-lactamase structures. The three refined KPC-2 molecules in the asymmetric unit are very similar to each other as reflected by the low rmsd of 0.29−0.34 Å for superposition of all Cα atoms (Figure 3B). The active site residues are also in very similar positions. Since these three molecules are very similar, we will be limiting our discussion and analysis to KPC-2 subunit A.

The structure of KPC-2 contains two subdomains generating a cleft resulting in an overall fold that is expectedly similar to that of other class A β-lactamases (Figure 3A). One of the subdomains is largely α-helical, whereas the other subdomain contains a five-stranded β-sheet flanked by α-helices. The cleft generated by these two subdomains harbors the active site containing the catalytic S70 residue and also harbors the deacylation water that is primed by interacting with E166 and N170 as well as S70 (Figure 4). The oxyanion hole formed by the backbone nitrogens of S70 and T237 is partially occluded by the side chain of S70 which is somewhat unusual for class A β-lactamases, which will be discussed later. Adjacent to S70 is residue C69 which is involved in a disulfide bond with C238. This disulfide bond is characteristic of class A carbapenemases, including NMC-A and SME (position 69 in class A enzymes usually is a M or other hydrophobic residue). Both conserved lysines (K73 and K234) are also present in the active site of KPC-2 as well as residue N132. The importance of these residues has been well established in class A β-lactamases (as reviewed in refs *27* and *28*). The entrance of the active site is flanked by W105 and R220 situated on opposite sides of the active site (Figure 4).

The active site contains a serendipitous, though interesting, finding in the form of a bound bicine buffer molecule. A bicine molecule is observed in the active site of all three KPC-2 molecules present in the asymmetric unit. The density is clearest for bicine in KPC-2 molecule A, with an average B factor for bicine of 25 Å^2, and its omit electron density is depicted in Figure 2B. The B factors for bicine in molecules B and C refined to somewhat higher average temperature factors of 36 and 45 Å^2, respectively. Bicine [di(hydroxyethyl)glycine] is a zwitterionic compound and contains a tertiary amine, a carboxyl group, and two hydroxyethyl groups (Figure 1). Its carboxyl moiety is involved in the majority of bicine's interactions in the active site by making hydrogen bonds with T235, T237, and S130, a salt bridge interaction with K234, a more distant ∼4 Å electrostatic interaction with R220, and some water-mediated interactions (Figure 4). The two hydroxyethyl moieties of bicine do not make direct hydrogen bonds with the protein (only a water-mediated interaction involving Wat3), but do provide hydrophobic interactions with W105. In addition, W105 could also be involved in a possible cation−π interaction of bicine's tertiary amine group (Figure 4). Preliminary kinetic analysis showed that bicine had some detectable though weak inhibitory effect on KPC-2 activity (measured up to 900 mM), and we therefore estimate its affinity is close to the buffer concentration of 100 mM in the crystallization experiment.

DISCUSSION

The structure of KPC-2 at 1.85 Å resolution provides a new understanding of the active site of a clinically important carbapenemase responsible for the widespread emergence of imipenem resistance in *K. pneumoniae* and other bacteria. Thus, the details revealed by our study are best appreciated in light of the structures of other serine class A β-lactamases. The mechanism that accounted for the carbapenemase phenotype in the class A β-lactamases, NMC-A and SME-1, was not precisely defined. The atomic structures of NMC-A and SME-1 when compared to TEM did not reveal a unifying structural basis for this enhanced catalytic activity (*12*, *13*). Nevertheless, the carbapenemase versus non-carbapenemase hydrolytic differences are dramatic since the former can hydrolyze carbapenems with great efficiency. The k_{cat}/K_m for imipenem hydrolysis is only 2.4 mM^{-1} s^{-1} for TEM-1 (*29*) and nondetectable for SHV-1 (*30*) yet is 100−4500-fold more efficient for carbapenemases with k_{cat}/K_m values of 300, 440, 1900, and 11300 mM^{-1} s^{-1} for KPC-2,

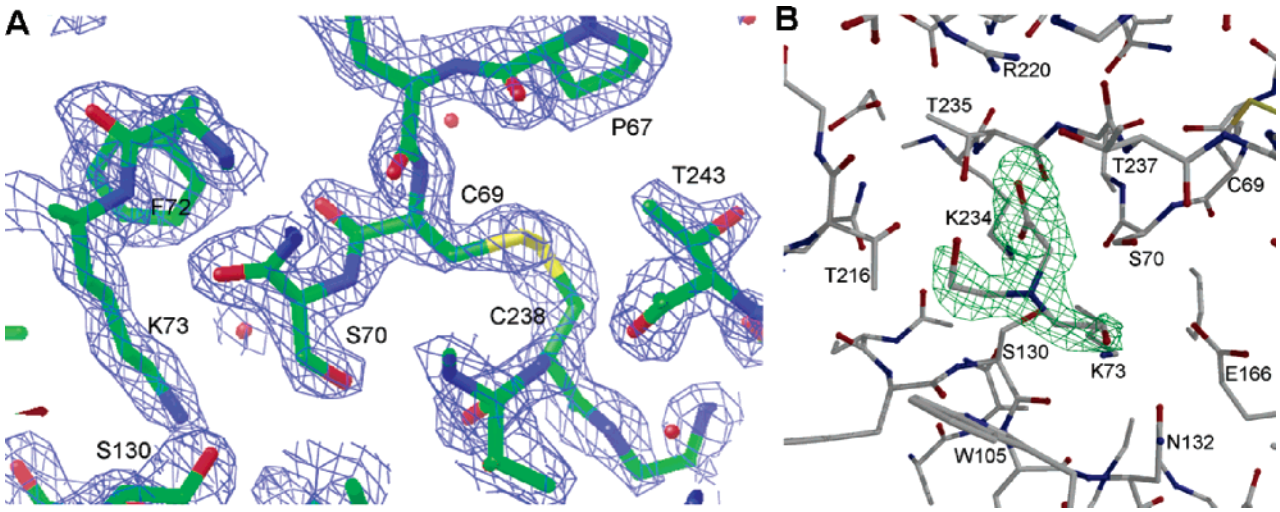

FIGURE 2: (A) Electron density of a region in the vicinity of the active site of KPC-2. The 1.85 Å resolution $|F_o| - |F_c|$ simulated annealing omit map contoured at 2.5σ is depicted. (B) Electron density for bicine in the active site of KPC-2. The $|F_o| - |F_c|$ simulated annealing omit electron density is contoured at 2.5σ.

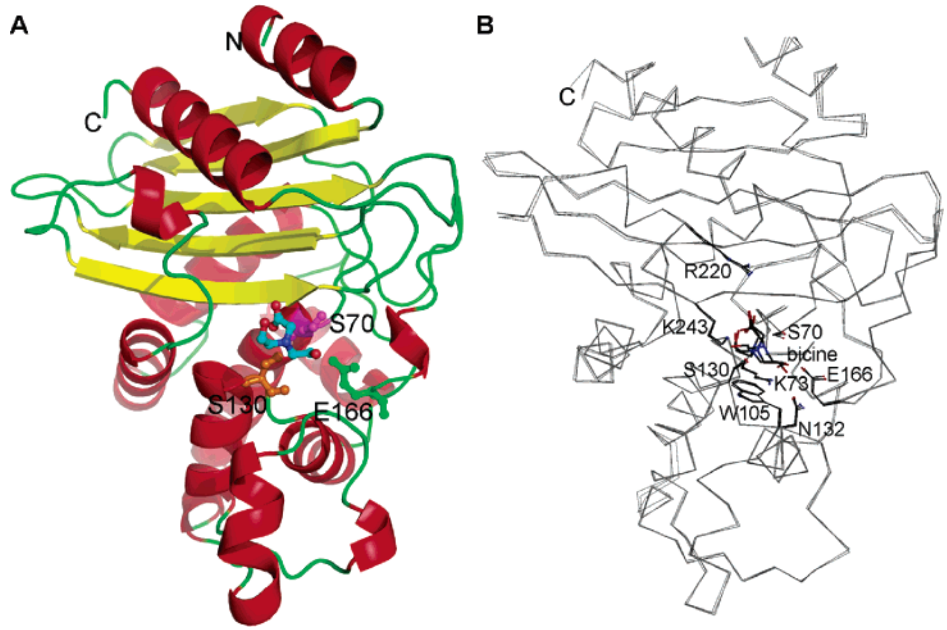

FIGURE 3: (A) Structure of KPC-2 β-lactamase. The secondary structure elements are colored yellow (β-strands), red (α-helices), and green (coil). To indicate the position of the active site, the positions of catalytic residues S70 (magenta), S130 (orange), and E166 (green) are labeled. Bicine is color-coded by atom type with the carbon atoms colored blue. (B) Superposition of three KPC-2 molecules present in the asymmetric unit. The three KPC-2 molecules are depicted in a Cα trace. Active site residues and bicine molecules are shown in stick representation and labeled accordingly.

SME-1, KPC-3, and NMC-A, respectively (*9*, *12*, *13*). A similar trend is observed for the cephamycin cefoxitin which is also hydrolyzed more efficiently by the carbapenemases, compared to TEM-1 and SHV-1 (*9*, *12*, *13*, *31*). Compared to these class A structures, the KPC-2 structure offers key insights into this novel kinetic behavior.

Superposition of the Cα atoms of KPC-2 onto NMC-A, SME-1, SHV-1, and TEM-1 results in rmsd values of 0.81, 0.80, 1.38, and 1.20 Å, respectively (for 256, 256, 235, and 240 superpositioned Cα atoms, respectively). Hence, KPC-2, SME-1, and NMC-A are quite similar in overall structure (Figure 5) with the largest deviations located distant from the active site [near loop residues 88 and 98 (Figure 5A)]. The sequence conservation shows a similar trend as KPC-2 is 52 and 54% identical in sequence with SME-1 and NMC-A yet only 38 and 36% identical with SHV-1 and TEM-1, respectively. Most of the active site residues are remarkably conserved between class A carbapenemases and non-carbapenemases except for a few residues that are different in the latter (Figure 5B). These residues are T237 (is a similar S in NMC-A and SME-1, yet is A in SHV-1 and TEM-1), H274 (M in SHV-1 and TEM-1), R220 (although an R side chain is present in SHV-1 and TEM-1, it comes from residue R244 instead), and T216 (M in SHV-1 and TEM-1). T237, H274, and R220 are all near the carboxyl moiety of bicine, suggesting an important role for these residues in that region of the active site, perhaps also interacting with the carboxyl moiety of the carbapenem and cephamycin substrates. Buried behind the active site is also the disulfide bond formed by C69 and C238 which is not present in SHV-1 and TEM-1. In addition to these residue differences, the active sites of the three carbapenemase

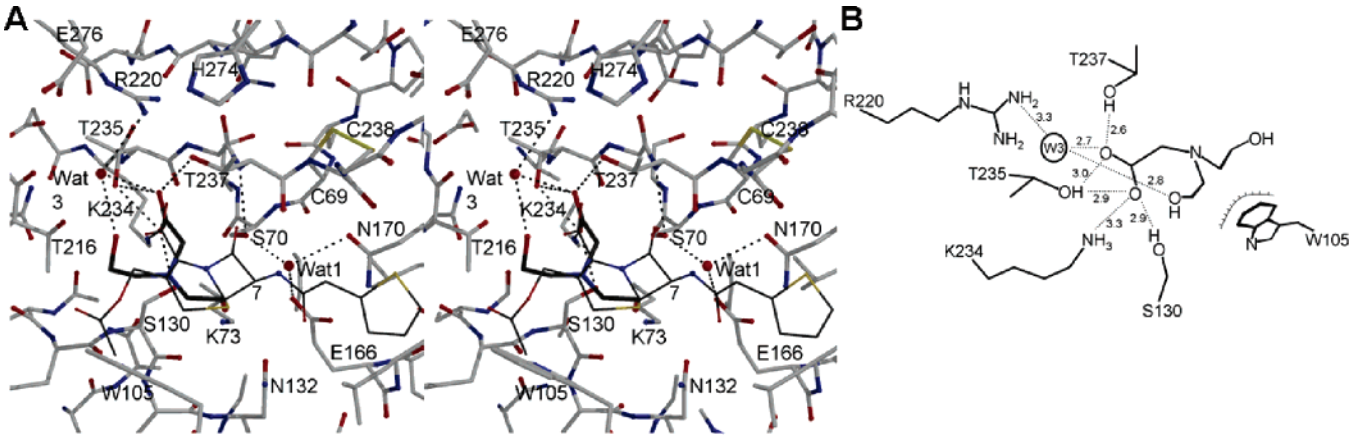

FIGURE 4: (A) Stereo figure depicting the active site of KPC-2 with bicine and a superpositioned cephalosporin. Bicine (thick dark sticks) and the cephalosporin cephalothin (thin dark sticks) are depicted. The position of cephalothin was obtained by superimposing the AmpC−cephalothin substrate complex [PDB entry 1KVL (*32*)] with KPC-2. The Cα atoms used in the superpositioning are KPC-2 residues 69−73, 132, and 235−238 on AmpC residues 63−67, 152, and 316−319 (superposition resulted in a rmsd of 0.67 Å for the 10 Cα atoms). Hydrogen bonds with bicine are shown as dashed lines. The carbon position of cephalothin in which cefoxitin has a 7α-OCH_3 substituent is labeled with the numeral 7. (B) Schematic diagram of interactions of bicine in the active site of KPC-2. Hydrogen bonds are depicted as dashed lines; van der Waals interactions with W105 are shown as a curved line with perpendicular lines. Hydrogen bond distances are given in angstroms.

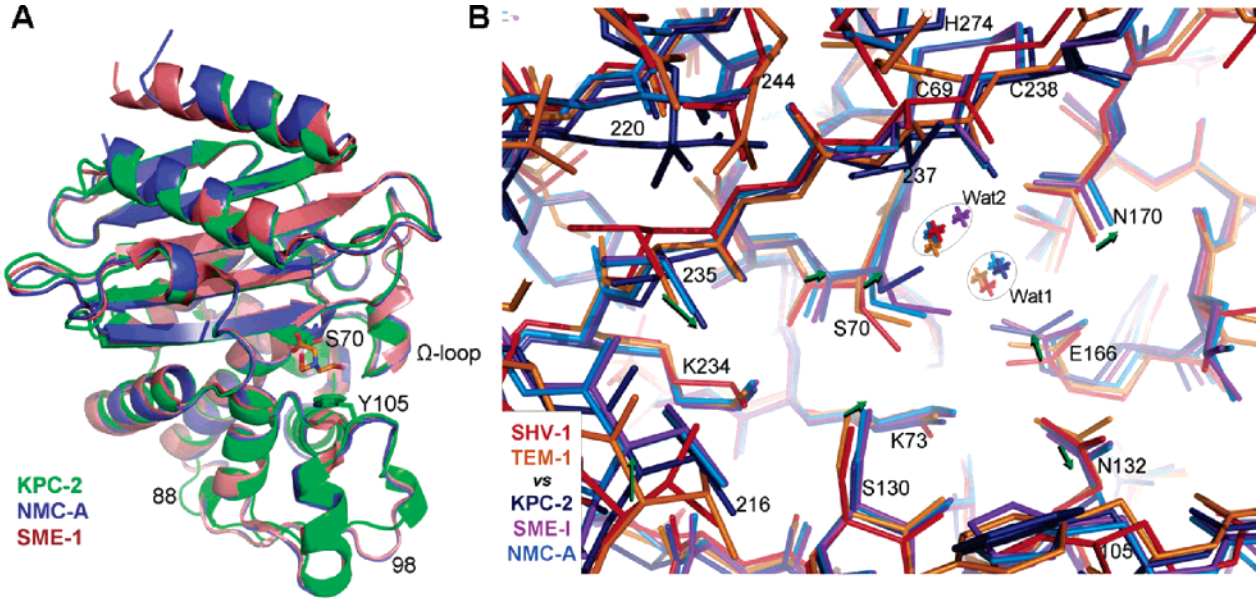

FIGURE 5: (A) Superposition of class A carbapenemases. The position of the active site is indicated by depicting residues S70 and Y105 as well as the flanking Ω-loop and bicine (in stick representation with cold colored carbon atoms). A couple of loops are deviating significantly between KPC-2 and NMC-A and SME-1 and are labeled (near residues 88 and 98). (B) Superposition of the active sites of the carbapenemases and non-carbapenemase β-lactamases. Superpositioned are KPC-2 (dark blue), NMC-A (light blue), and SME-1 (magenta) and non-carbapenemases SHV-1 (red) and TEM-1 (orange). Green arrows highlight common shifts comparing the carbapenemase and non-carbapenemase structures. Two key clusters of waters are circled: the deacylation water primed by E166 and N170 (Wat1) and the water occupying the oxyanion hole formed by backbone nitrogens of residues 70 and 237 (Wat2). The following 11 Cα atoms were used to superposition the active sites of the β-lactamases: 69, 70, 73, 105, 130, 132, 166, 170, 234, 236, and 237.

structures reveal a number of conserved shifts with respect to the non-carbapenemases, SHV-1 and TEM-1 β-lactamases (Figure 5B and Tables 2 and 3), suggesting a functional significance. These shifts are significant since they are all larger than the 0.2 Å ESD coordinate errors reported for these structures (coordinate errors are listed in Table 2).

Comparing SHV-1 and TEM-1 versus KPC-2, NMC-A, and SME-1, we observed that the following active site alterations are unique among the carbapenemases. First, the decreased length of the pocket containing two water molecules, Wat1 (deacylation water) and Wat2 (occupies temporarily the oxyanion hole), stands out as a distinctive feature among the carbapenemases. This length of this pocket is determined by the position of the OE2 atom of E166 and the N atom of residue 237 which are located on opposite ends of this pocket, each making one hydrogen bond with one of the water molecules. This space reduction in pocket length is quantified by the observed 0.5−1.9 Å shortening of the T237 N−E166 OE2 distance (Table 2). Residue E166 in itself is shifted by 0.3−0.9 Å in the carbapenemases compared to non-carbapenemases (Table 3). This pocket is flanked by S70 whose relative repositioning of 0.5−0.8 Å in carbapenemases (Table 3) further decreases the size of the pocket for the two waters as evidenced by the 0.5−1.4 Å reduction of the S70 CA−residue 237 CA distance in carbapenemases relative to the non-carbapenemases

Table 2: Active Site Distance Changes of Carbapenemases and Non-Carbapenemases

	resolution (Å)	ESD coordinate error using Luzzati (Å)	distance (Å)		
			T237 N−E166 OE2	N170 CD−N132 CD	S70 CA−237 CA
carbapenemases					
KPC-2	1.85	0.17	7.1	7.3	5.8
NMC-A	1.64	0.18	8.1	7.5	6.2
SME-1	2.1	ND[a]	7.8	7.3	6.3
non-carbapenemases					
SHV-1	1.98	0.2	9.0	6.7	7.2
TEM-1	1.9	0.17	8.6	6.6	6.8

[a] The coordinate error is not listed for SME-1 but is likely similar to the value of 0.2 Å for SHV-1 since their resolution and refined R and R_{free} values are similar.

Table 3: Relative Shifts in Active Site Residues of Carbapenemases Compared to Non-Carbapenemases

	shift (Å) relative to SHV-1 (and TEM-1)						
	S130 OG	T235 OG1	S70 CA	N170 CA	E166 CA	N132 CA	T/V216 CA
KPC-2	0.6 (0.5)[a]	1.7 (1.0)	0.8 (0.9)	0.6 (0.5)	0.9 (0.9)	0.5 (0.5)	1.0 (0.8)
NMC-A	0.7 (0.4)	1.2 (0.6)	0.5 (0.5)	0.5 (0.4)	0.4 (0.3)	0.8 (0.7)	1.5 (1.3)
SME-1	0.8 (0.6)	1.2 (0.6)	0.7 (0.7)	0.3 (0.2)	0.6 (0.6)	0.8 (0.7)	1.5 (1.3)

[a] Carbapenemase shifts relative to the TEM-1 structure are all listed in parentheses.

(Table 2). S70 is therefore positioned less deep in the active site in carbapenemases. Second, there is increase in the space adjacent to the water pocket created by concurrent shifts of N132 and N170 in roughly opposite directions. This is measured by the 0.6−0.9 Å increase in distance between the CD atoms of N170 and N132 for carbapenemases (Table 2). Third, a reoriented carbonyl group of C238 due to the C69−C238 disulfide bond and a one-residue insertion after C238 is observed. Last, the 0.4−0.8 Å relative shift of the OG atom of S130, the 0.6−1.7 Å relative shift of the OG1 atom of Thr235, and the 0.8−1.5 Å relative shift of residue T216 are also unique features among the carbapenemases (Table 3).

The change listed in our first observation result in a decreased space for the usually present waters, Wat1 and Wat2, and has a remarkable effect on the number of waters present in the active sites of the carbapenemases depending on the position of S70. In KPC-2, the side chain of S70 partially blocks the oxyanion hole, and this structure therefore lacks Wat2 (Figure 5B). In SME-1, S70 points into the direction of the deacylation water cavity and SME-1 therefore lacks Wat1 yet does harbor the oxyanion hole Wat2. Only NMC-A has both Wat1 and Wat2 present in the active site since S70 has shifted in NMC-A somewhat less than in the other two carbapenemases (Figure 5B). In non-carbapenemases such as SHV-1 and TEM-1, these waters are always present in their apo structures (Figure 5B). Since both cavities need to be available during catalysis (Wat2 cavity for the carbonyl oxygen atom of carbapenem during acylation and Wat1 for subsequent deacylation), we speculate that S70 adopts different conformations during catalysis to free these cavities in a successive manner. Increasing the level of S70 movement is likely made possible by the more protruding S70 position in the active sites of carbapenemases (Figure 5B).

The changes listed above have potential consequences for the ability of carbapenemases to hydrolyze imipenem and cefoxitin. First, we hypothesize that having S70 positioned in a more shallow position means that the β-lactam ring of carbapenems does not have to enter the catalytic cleft as deeply which would normally be sterically hampered by the 6α-substituent of carbapenems or the 7α-substituent of cephamycins. To illustrate this, we have used the structure of the cephalothin−AmpC Michaelis−Menten substrate complex and superimposed it onto KPC-2 (Figures 4 and 6) (*32*). Although AmpC is a class C β-lactamase, it is to our knowledge the only known substrate−serine-β-lactamase complex, and many key active site residues are conserved between class C and class A β-lactamases (i.e., S70, K73, N132, K234, G236, T235, and A/T237). This substrate complex superposition provides a good starting point for understanding the significance of the observed shifts with respect to carbapenems and cephamycin hydrolysis, in particular since cephalothin is structurally related to cefoxitin as it lacks only the 7α-O-CH_3 moiety (Figure 1).

The superposition reveals that the carboxyl moiety of cephalothin is in a position similar to that of the carboxyl moiety of bicine, an observation that also strengthens the relevance of bicine's active site interactions. The observed shift of S70 being positioned less deep in the active site would allow the cefoxitin to approach the active site at a slightly different angle such that its 7α-O-CH_3 moiety shifts to a wider area of the active site to minimize steric clashes (Figure 6A). In addition to this approximate in-plane reorientation of cefoxitin, cefoxitin is postulated to undergo an additional movement perpendicular to the first rotation (Figure 6B). This second rotation is likely due to the concerted shifts of S130 and T235 (Figure 5B) which are postulated to provide key anchoring hydrogen bonds with the carboxyl group of cefoxitin as extrapolated from the initial superposition of the AmpC complex with KPC-2 (Figure 4), the bicine interactions with KPC-2, and the fact that the carboxyl moiety of cefoxitin forms a hydrogen bond with T316 in AmpC which is the structural equivalent of T235 in KPC-2 (*32*). In addition, the carboxyl moiety of the inhibitor 6α-(hydroxypropyl)penicillanate when bound to NMC-A forms similar interactions with T235, S237, S130, and K73, although this a covalent acyl-enzyme complex and not a Michaelis−Menten complex (*14*). Both S130 and T235 are shifted such that the carboxyl group and the rest of the

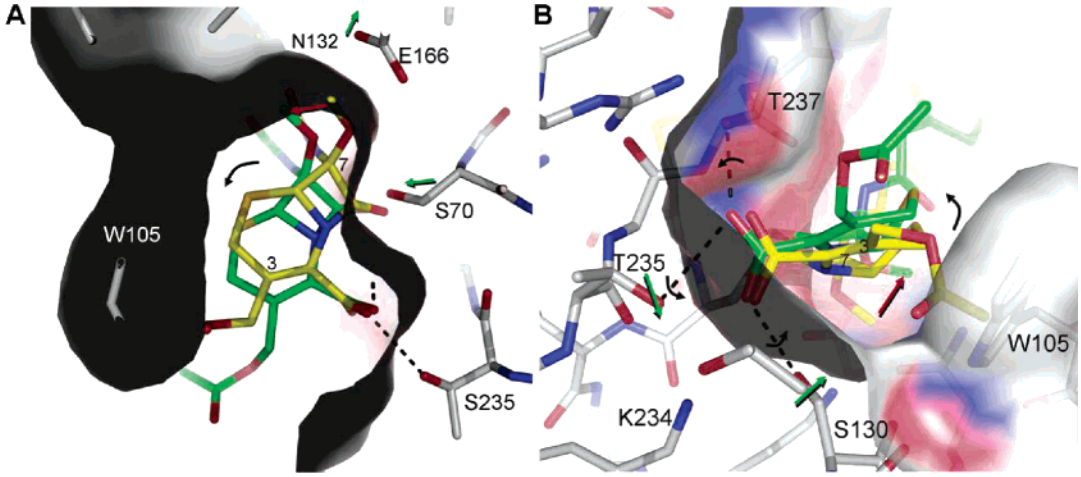

FIGURE 6: Active site adjustments of KPC-2 and their postulated role in accommodating cefoxitin. The initial position of cefoxitin is obtained after superposition of the KPC-2 and AmpC−cephalothin active sites and addition of the O-CH_3 moiety to cephalothin's 7α position to form cefoxitin (yellow). Cefoxitin was reoriented (green), which was guided by observed active site readjustments, to alleviate steric clashes with its 7α-O-CH_3 moiety. In addition, the conformation of its 3-substituent was adjusted as well to alleviate steric clashes. (A) View from the bottom of the active site. Observed key shifts in KPC-2 relative to non-carbapenemases are denoted with green arrows. The shift of residue N132 (faint in background) likely provides additional space for the 7α-O-CH_3 substituent of cefoxitin. The observed shift of S70 to a more outward position allows a less deep active site penetration of the *β*-lactam ring of cefoxitin. This could result in a ligand reorientation (curved arrow) such that the 7α-O-CH_3 moiety shifts (red arrow), thereby further alleviating steric clashes. (B) Side view obtained by an approximate 90° rotation along the horizontal axis compared to the view in panel A. This view shows the postulated effects of the concerted shifts of T235 and S130 (green arrows) in possibly reorienting the carboxyl moiety (in the direction of the small curved arrows), and the rest of cefoxitin (in the direction of the larger curved arrow), in a counterclockwise fashion to reposition its 7α-O-CH_3 group (red arrow) to a wider region of the active site to prevent steric clashes. The presence of the Ser/Thr at position 237 in carbapenemases could provide an additional stabilizing hydrogen bond for the carboxyl moiety of cefoxitin to aid in this postulated reorientation (SHV-1 and TEM-1 have an Ala at this position). The described shifts and reorientation for cefoxitin are also postulated to occur for carbapenems.

ligand might undergo a counterclockwise rotation as indicated in Figure 6B. The active site is wide enough to accommodate such a reorientation of cefoxitin which likely results in additional space for the 7α-OCH_3 group. An interesting observation is that the carboxyl moiety of bicine, and presumably also cefoxitin, also interacts with T237, in addition to S130 and T235 (Figures 4 and 6B). The importance of the O*γ* atom at position 237 has been noted since only a S or T at this position could maintain carbapenemase activity (*16*, *33*). Loss of this hydroxyl in SME-1 leads to a 5-fold decrease in k_{cat} for imipenem hydrolysis (*33*). This suggests that the O*γ* atom of residue 237 could indeed be critical for orienting cefoxitin, and imipenem, via interaction with their carboxyl moieties, thereby improving the catalytic efficiency of their hydrolysis.

Residues in the immediate vicinity of T237 are R220 and H274 with which it forms a 2.7 Å hydrogen bond and a 3.4 Å van der Waals interaction, respectively. As noted above, all three residues are changed in SHV-1 and TEM-1, further emphasizing the importance of this region for carbapenemase activity. R220 provides, in addition to its hydrogen bond with T237, an ~4 Å electrostatic interaction and a water-mediated interaction with the carboxyl moiety of bicine. In KPC-3, residue H274 is mutated to a tyrosine which leads to an ~6-fold enhancement in k_{cat}/K_m for imipenem compared to that for KPC-2 (and KPC-1) (*9*). Both R220 and H274 are therefore postulated to have an effect on substrate binding either electrostatically or indirectly via correctly positioning T237 and/or the Wat3 water molecule (see Figure 4). In summary, the ability of carbapenemases to accommodate α-substituents present in carbapenems and cephamycins is postulated to result from multiple active site adjustments so that these substrates can access the active site in a somewhat different orientation, thereby repositioning their α-substituents to a wider part of the active site. Shifts of nearby N170 and N132 in particular likely provide additional room as well. The active site shifts are supported by conserved residue changes in carbapenemases, in particular, near the postulated carboxyl binding site, to provide additional direct or indirect interaction strength.

The perimeter of the active site of carbapenemases contains an additional residue that merits consideration. This residue is W105 which in the SME-1 carbapenemase and other class A *β*-lactamases has been found to have a strong preference for aromatic residues (*16*). This aromatic residue at position 105 could provide favorable stacking interactions with the carbapenem substrate in the Michaelis−Menten complex (*34*, *35*), which is also evident from the cefoxitin superposition (Figures 4 and 6). SME-1 and NMC-A contain a histidine at this position, whereas KPC-2 contains a tryptophan; however, even non-carbapenemases usually have an aromatic residue at this position (Figure 5B). It is possible that either a H or W at this position could provide a hydrogen bond with the substrate in addition to the postulated stacking interaction. Residues T217 and P104 (F in NMC-A and Y in SME-1) are located a bit more distant compared to W105 yet could potentially play a role in interacting with the different substituents of carbapenems and cephamycins.

In addition to the postulated changes in carbapenemases to reorient the carbapenem and cephamycin substrates such that their α-substituents can be accommodated in a productive Michaelis−Menten complex, carbapenemases have also evolved so that they are not inhibited by long-lived reaction intermediates of these substrates. For example, TEM-1 has been shown to react with imipenem, albeit with low affinity. However, imipenem's acyl-enzyme intermediate becomes

trapped in the active site of TEM-1 due to displacement of the deacylation water and the repositioning of the β-lactam carbonyl outside the oxyanion hole, interacting with S130 instead (*36*). This nonproductive deacylation configuration is likely due to imipenem's 6α-hydroxyethyl moiety which makes a hydrogen bond with N132. In the carbapenemases, such a trapped covalently bound imipenem configuration is likely avoided by the simultaneous shift of N132 and S70 in somewhat opposite directions, limiting such N132-mediated intermediate-stabilizing interactions and favoring efficient carbapenem hydrolysis (Figure 5B). Thus, carbapenemases are not only able to accommodate the bulkier carbapenems in the initial binding step but also avoid being inhibited by undesired long-lived intermediates. This could be aided by the postulated increased flexibility of S70. The S70 flexibility could even have a role in allowing the carbapenems and cephamycins to readjust to accommodate the α-substituent group during the initial Michaelis−Menten complex.

In summary, we present the structure of KPC-2, a clinically important carbapenemase present in *K. pneumoniae* and other nosocomial pathogens. This analysis provides insight into the unique properties of this β-lactamase and explains its ability to hydrolyze cephamycins and carbapenems; the latter constitute our "last line" of defense against β-lactam resistant bacteria. Our findings also demonstrate that apparently subtle changes in active site topology (0.5−0.8 Å relocation of the catalytic S70) and other shifts in conserved amino acid positions in class A β-lactamases have a profound effect on substrate specificity, likely by allowing the substrates to bind at a slightly different angle to alleviate steric hindrance. The process of new β-lactam drug discovery must anticipate these unexpected consequences of protein remodeling. It is important to recall that the carboxyl moiety of bicine in KPC-2 is in a position almost identical to that of the carboxyl moiety of our previously designed SA2-13 inhibitor when bound to SHV-1 (*37*). This suggests that the inhibition strategy of *trans*-enamine stabilization using carboxyl-linker penam sulfone derivatives could potentially be applicable to carbapenemases.

ACKNOWLEDGMENT

We thank Dr. Fred Tenover for the pBR322-catI-blaKPC-2 construct. We thank the personnel at SBC beamline 19BM at Advanced Photon Source for help with data collection and use of their facilities.

REFERENCES

1. Babic, M., Hujer, A. M., and Bonomo, R. A. (2006) What's new in antibiotic resistance? Focus on β-lactamases, *Drug Resist. Updates 9*, 142−156.
2. Paterson, D. L. (2006) Resistance in gram-negative bacteria: Enterobacteriaceae, *Am. J. Infect. Control 34*, S20−S28.
3. Bratu, S., Mooty, M., Nichani, S., Landman, D., Gullans, C., Pettinato, B., Karumudi, U., Tolaney, P., and Quale, J. (2005) Emergence of KPC-possessing *Klebsiella pneumoniae* in Brooklyn, New York: Epidemiology and recommendations for detection, *Antimicrob. Agents Chemother. 49*, 3018−3020.
4. Woodford, N., Tierno, P. M., Jr., Young, K., Tysall, L., Palepou, M. F., Ward, E., Painter, R. E., Suber, D. F., Shungu, D., Silver, L. L., Inglima, K., Kornblum, J., and Livermore, D. M. (2004) Outbreak of *Klebsiella pneumoniae* producing a new carbapenem-hydrolyzing class A β-lactamase, KPC-3, in a New York Medical Center, *Antimicrob. Agents Chemother. 48*, 4793−4799.
5. Bratu, S., Landman, D., Haag, R., Recco, R., Eramo, A., Alam, M., and Quale, J. (2005) Rapid spread of carbapenem-resistant *Klebsiella pneumoniae* in New York City: A new threat to our antibiotic armamentarium, *Arch. Intern. Med. 165*, 1430−1435.
6. Pope, J., Adams, J., Doi, Y., Szabo, D., and Paterson, D. L. (2006) KPC type β-lactamase, rural Pennsylvania, *Emerging Infect. Dis. 12*, 1613−1614.
7. Naas, T., Nordmann, P., Vedel, G., and Poyart, C. (2005) Plasmid-mediated carbapenem-hydrolyzing β-lactamase KPC in a *Klebsiella pneumoniae* isolate from France, *Antimicrob. Agents Chemother. 49*, 4423−4424.
8. Navon-Venezia, S., Chmelnitsky, I., Leavitt, A., Schwaber, M. J., Schwartz, D., and Carmeli, Y. (2006) Plasmid-mediated imipenem-hydrolyzing enzyme KPC-2 among multiple carbapenem-resistant *Escherichia coli* clones in Israel, *Antimicrob. Agents Chemother. 50*, 3098−3101.
9. Alba, J., Ishii, Y., Thomson, K., Moland, E. S., and Yamaguchi, K. (2005) Kinetics study of KPC-3, a plasmid-encoded class A carbapenem-hydrolyzing β-lactamase, *Antimicrob. Agents Chemother. 49*, 4760−4762.
10. Ambler, R. P., Coulson, A. F., Frere, J. M., Ghuysen, J. M., Joris, B., Forsman, M., Levesque, R. C., Tiraby, G., and Waley, S. G. (1991) A standard numbering scheme for the class A β-lactamases, *Biochem. J. 276* (Part 1), 269−270.
11. Yigit, H., Queenan, A. M., Anderson, G. J., Domenech-Sanchez, A., Biddle, J. W., Steward, C. D., Alberti, S., Bush, K., and Tenover, F. C. (2001) Novel carbapenem-hydrolyzing β-lactamase, KPC-1, from a carbapenem-resistant strain of *Klebsiella pneumoniae*, *Antimicrob. Agents Chemother. 45*, 1151−1161.
12. Swaren, P., Maveyraud, L., Raquet, X., Cabantous, S., Duez, C., Pedelacq, J. D., Mariotte-Boyer, S., Mourey, L., Labia, R., Nicolas-Chanoine, M. H., Nordmann, P., Frere, J. M., and Samama, J. P. (1998) X-ray analysis of the NMC-A β-lactamase at 1.64-Å resolution, a class A carbapenemase with broad substrate specificity, *J. Biol. Chem. 273*, 26714−26721.
13. Sougakoff, W., L'Hermite, G., Pernot, L., Naas, T., Guillet, V., Nordmann, P., Jarlier, V., and Delettre, J. (2002) Structure of the imipenem-hydrolyzing class A β-lactamase SME-1 from *Serratia marcescens*, *Acta Crystallogr. D58*, 267−274.
14. Mourey, L., Miyashita, K., Swaren, P., Bulychev, A., Samama, J. P., and Mobashery, S. (1998) Inhibition of the NMC-A β-lactamase by a penicillanic acid derivative and the structural bases for the increase in substrate profile of this antibiotic resistance enzyme, *J. Am. Chem. Soc. 120*, 9382−9383.
15. Majiduddin, F. K., and Palzkill, T. (2003) Amino acid sequence requirements at residues 69 and 238 for the SME-1 β-lactamase to confer resistance to β-lactam antibiotics, *Antimicrob. Agents Chemother. 47*, 1062−1067.
16. Majiduddin, F. K., and Palzkill, T. (2005) Amino acid residues that contribute to substrate specificity of class A β-lactamase SME-1, *Antimicrob. Agents Chemother. 49*, 3421−3427.
17. Yigit, H., Queenan, A. M., Rasheed, J. K., Biddle, J. W., Domenech-Sanchez, A., Alberti, S., Bush, K., and Tenover, F. C. (2003) Carbapenem-resistant strain of *Klebsiella oxytoca* harboring carbapenem-hydrolyzing β-lactamase KPC-2, *Antimicrob. Agents Chemother. 47*, 3881−3889.
18. Hujer, A. M., Hujer, K. M., and Bonomo, R. A. (2001) Mutagenesis of amino acid residues in the SHV-1 β-lactamase: The premier role of Gly238Ser in penicillin and cephalosporin resistance, *Biochim. Biophys. Acta 1547*, 37−50.
19. Otwinowski, Z., and Minor, W. (1997) Processing of X-ray diffraction data collected in oscillation mode, *Methods Enzymol. 276*, 307−326.
20. McCoy, A. J., Grosse-Kunstleve, R. W., Storoni, L. C., and Read, R. J. (2005) Likelihood-enhanced fast translation functions, *Acta Crystallogr. D61*, 458−464.
21. Murshudov, G. N., Vagin, A. A., and Dodson, E. J. (1997) Refinement of macromolecular structures by the maximum-likelihood method, *Acta Crystallogr. D53*, 240−255.
22. Emsley, P., and Cowtan, K. (2004) Coot: Model-building tools for molecular graphics, *Acta Crystallogr. D60*, 2126−2132.
23. Yeates, T. O. (1997) Detecting and overcoming crystal twinning, *Methods Enzymol. 276*, 344−358.
24. Brunger, A. T., Adams, P. D., Clore, G. M., DeLano, W. L., Gros, P., Grosse-Kunstleve, R. W., Jiang, J. S., Kuszewski, J., Nilges, M., Pannu, N. S., Read, R. J., Rice, L. M., Simonson, T., and Warren, G. L. (1998) Crystallography & NMR system: A new

software suite for macromolecular structure determination, *Acta Crystallogr. D54*, 905−921.
25. van den Akker, F., and Hol, W. G. (1999) Difference density quality (DDQ): A method to assess the global and local correctness of macromolecular crystal structures, *Acta Crystallogr. D55* (Part 1), 206−218.
26. Laskowski, R. A., MacArthur, M. W., Moss, D. S., and Thornton, J. M. (2001) PROCHECK: A program to check the stereochemical quality of protein structures, *J. Appl. Crystallogr. 26*, 283−291.
27. Matagne, A., Lamotte-Brasseur, J., and Frere, J. M. (1998) Catalytic properties of class A β-lactamases: Efficiency and diversity, *Biochem. J. 330* (Part 2), 581−598.
28. Minasov, G., Wang, X., and Shoichet, B. K. (2002) An ultrahigh resolution structure of TEM-1 β-lactamase suggests a role for Glu166 as the general base in acylation, *J. Am. Chem. Soc. 124*, 5333−5340.
29. Raquet, X., Lamotte-Brasseur, J., Bouillenne, F., and Frere, J. M. (1997) A disulfide bridge near the active site of carbapenem-hydrolyzing class A β-lactamases might explain their unusual substrate profile, *Proteins 27*, 47−58.
30. Poirel, L., Heritier, C., Podglajen, I., Sougakoff, W., Gutmann, L., and Nordmann, P. (2003) Emergence in *Klebsiella pneumoniae* of a chromosome-encoded SHV β-lactamase that compromises the efficacy of imipenem, *Antimicrob. Agents Chemother. 47*, 755−758.
31. Neu, H. C. (1983) β-Lactamase stability of cefoxitin in comparison with other β-lactam compounds, *Diagn. Microbiol. Infect. Dis. 1*, 313−316.
32. Beadle, B. M., Trehan, I., Focia, P. J., and Shoichet, B. K. (2002) Structural milestones in the reaction pathway of an amide hydrolase: Substrate, acyl, and product complexes of cephalothin with AmpC β-lactamase, *Structure 10*, 413−424.
33. Sougakoff, W., Naas, T., Nordmann, P., Collatz, E., and Jarlier, V. (1999) Role of ser-237 in the substrate specificity of the carbapenem-hydrolyzing class A β-lactamase Sme-1, *Biochim. Biophys. Acta 1433*, 153−158.
34. Doucet, N., De Wals, P. Y., and Pelletier, J. N. (2004) Site-saturation mutagenesis of Tyr-105 reveals its importance in substrate stabilization and discrimination in TEM-1 β-lactamase, *J. Biol. Chem. 279*, 46295−46303.
35. Bethel, C. R., Hujer, A. M., Hujer, K. M., Thomson, J. M., Ruszczycky, M. W., Anderson, V. E., Pusztai-Carey, M., Taracila, M., Helfand, M. S., and Bonomo, R. A. (2006) Role of Asp104 in the SHV β-lactamase, *Antimicrob. Agents Chemother. 50*, 4124−4131.
36. Maveyraud, L., Mourey, L., Kotra, L. P., Pedelacq, J. D., Guillet, V., Mobashery, S., and Samama, J. P. (1998) Structural basis for clinical longevity of carbapenem antibiotics in the face of challenge by the common class A β-lactamases from the antibiotic-resistant bacteria, *J. Am. Chem. Soc. 120*, 9748−9752.
37. Padayatti, P. S., Sheri, A., Totir, M. A., Helfand, M. S., Carey, M. P., Anderson, V. E., Carey, P. R., Bethel, C. R., Bonomo, R. A., Buynak, J. D., and van den, A. F. (2006) Rational design of a β-lactamase inhibitor achieved via stabilization of the trans-enamine intermediate: 1.28 Å crystal structure of wt SHV-1 complex with a penam sulfone, *J. Am. Chem. Soc. 128*, 13235−13242.

BI700300U